BIL chamber prototype assembly in Protvino. Tools, procedure and some test results.

A.Borisov, E.Borisov, V.Goryatchev, R.Fakhroutdinov, A.Kojine, V.Rybachenko, V.Startsev, V.Tumakov, A.Vovenko

Institute for High Energy Physics
Protvino, 142284, Moscow region, Russia

1 Introduction

In this note we describe the assembling procedure, tools and some test results of full-scale BIL chamber prototype completed at IHEP of Protvino in November 1996.

The chamber was intended for DATCHA setup at CERN but its design followed the BIL chamber requirements concept developed by the ATLAS Muon Working Group and described in the ATLAS Technical Proposal [1]. Main design aims for the chamber are 20 μm wire location at the ends of drift tube and wire-tube concentricity better than 100 μm everywhere.

The chamber has two multilayers (fig.1) consisting of 3 layers of 30 mm diameter aluminium tubes glued together. Spacer (support) structure of 150 mm height separates multilayers. Each layer except for one marked by digit '5' in fig.1 consists of 96 tubes, 2560 mm long. There are 95 tubes in layer 5. There are cutouts at corners of one multilayer for pass of projective alignment rays. The tubes in the cutouts are 36 cm shorter, they are shown as hatched cycles in fig.1.

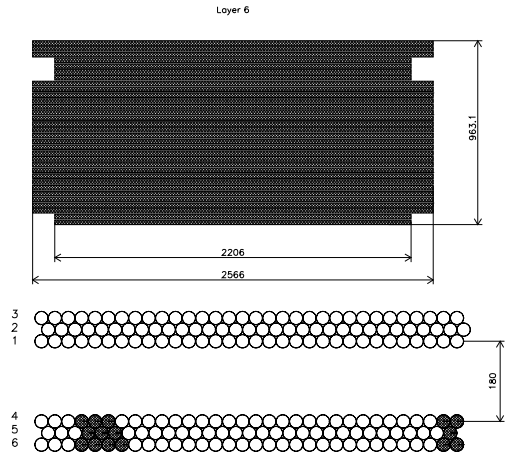

Figure 1: Scheme of the BIL chamber.

More than 200 tubes were done and tested for the chamber. Some results of tube tests are given separately in [2].

For the chamber assembling we adopted the layered scheme initially proposed by Frascati group [3].

In the following brief end plug description will be done, also we shall describe tube stacking comb design, spacer support structure, assembling procedure, some results of RASNIK measurements during the chamber assembling, our view on X-tomography data, some results of tests after installation of the chamber into the DATCHA pit.

2 End plug

All tubes of the chamber were equipped by end plugs designed and produced at IHEP of Protvino. During the chamber production we were limited by temporal frame of DATCHA setup schedule and due to this reason we did not develop end plug for mass-production. But we believe, that our end plug fulfills the most functional requirements given for ATLAS MDT. The main features of the end plug (fig.2) were given in [4] but we not sure that this paper is available now and repeat briefly the end plug description.

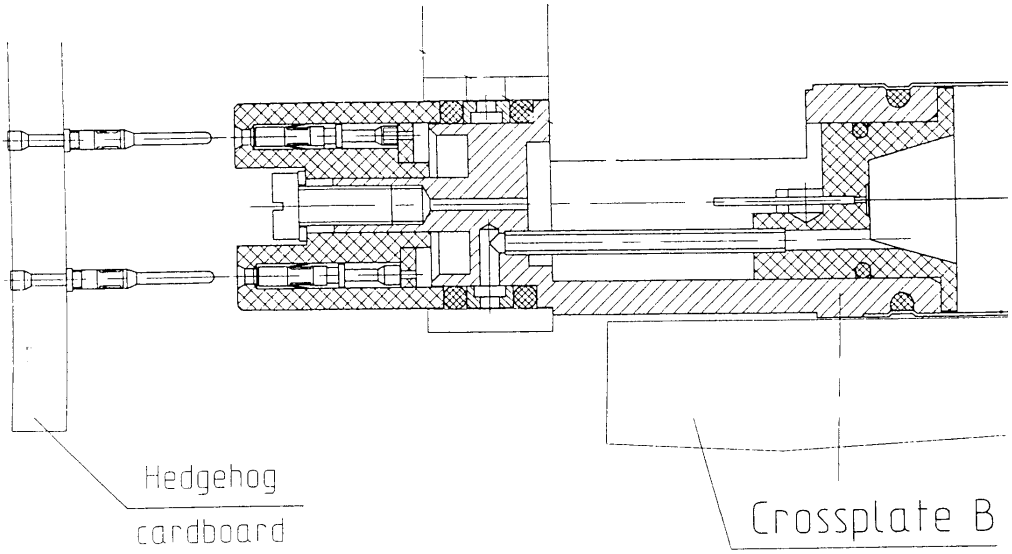

Figure 2: End plug of the chamber read-out side.

The basic concepts of the end plug are follows:

1. wire location is done by small hole in the end plug;
2. wire is fixed by mechanical crimping;
3. end plug in tube is fixed by gas crimping;
4. end plug has precise reference surface for positioning a tube in a layer;
5. gas tightness is guaranteed mainly by O-rings plus epoxy glue;
6. any plastic pipes for connection with gas manifold are excluded.

Main part of the end plug is an aluminium body with precisely machined outer diameter 30.1 mm inside of which a plexiglass insulator is inserted. A small brass disk with

laser drilled hole is glued to the insulator on internal surface of the end plug. This is a wire locator. The hole diameter is $50^{+10}\mu$m and its eccentricity is less than 10 μm as it was controlled during manufacturing. Such tolerances were confirmed by independent X-ray measurements. We were able to check about 14% of tubes by our X-ray scanner and found that mean wire eccentricity is 12 μm with RMS 6.7 μm. For Y and Z wire offset we obtained about zero mean value with RMS 10.3 and 8.5 μm accordingly [2]. So, we solved the problem of wire location with respect to the tube reference surface.

Fixation of 50 μm W(Au) wire was done by crimping in copper tube with inner diameter 0.27 mm and outer one 1.0 mm. Our many years experience with such manner of wire fixation let us to tell about its high reliability.

Fixation of the end plug in a tube was performed by gas crimping of tube surface over O-ring by pressure 140-160 atm. Fixation is reliable and gas-tight, but we detected some increasing of tube diameter at boundaries of crimping region. We suppose the deformation was caused by O-ring. The problem must be investigated in future.

There is a special tail part of the end plug. It provides parallel connection of all tubes to a gas manifold within of one multilayer without any plastic pipes. It is not so easy to attach the manifold to the chamber, but idea is useful and may be developed further.

One problem which was not solved properly in our end plug is gas tightness of its internal pieces (insulator and steel gas pipe) made by O-rings and epoxy glue. After shipment of the chamber to CERN we detected leakage rate about 15 bar·l/hour and could reduce it to 1 bar·l/hour at 3 bar over pressure after some additional gluing of end plugs. The end plug internal sealing made by O-rings of bad quality with epoxy glue gave the most leakage. In future we should like to avoid the epoxy glue using for gas tightness as much as possible.

3 Comb for tube stacking in a layer

The comb task is a location of tubes during a layer gluing. There are two approaches to construction of such combs. One is based on groves cylindrical or triangle shape developed by Seatle [5] and MPI [6] groups. Frascati group [7] proposed the using of precise rods array for tube location in a layer. We continued the rods comb idea to its logical end and developed the comb with balls. The advantages are evident: balls of any diameters are available from bearing industry; balls do not require any machining, they have hard, well polished surface with excellent tolerances, the balls permit to overcome a question about collinearity tubes and comb groves or rods.

For our comb we used $16.002^{+0.001}$ mm diameter balls with difference from ideal sphere less than 1 μm. Schematically the comb is shown in fig.3.

The comb base is an aluminium plate 1450x260x20 mm^3 at top of which there is a row of 47 balls glued by epoxy. Balls centers are 2 mm higher than plate top level. Sizes presented at the drawing correspond to 18°C. At such temperature comb must separate tubes in a layer with pitch 30.1 ± 0.005 mm.

Plates for combs were machined without high precision. The pits for balls also have not tight tolerances and their diameter is about 1 mm larger then balls one. Positioning of the balls on plate was performed with precisely machined tool (fig.4).

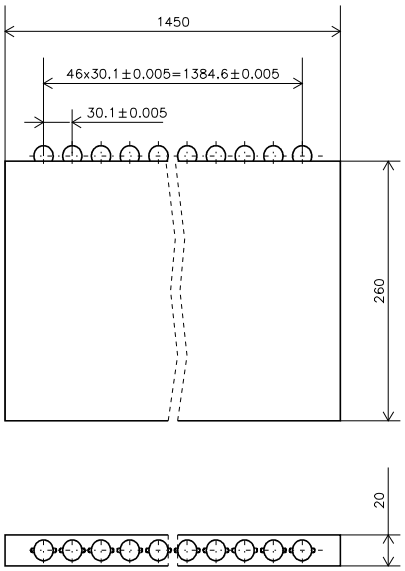

Figure 3: Ball comb for stacking tubes in a layer.

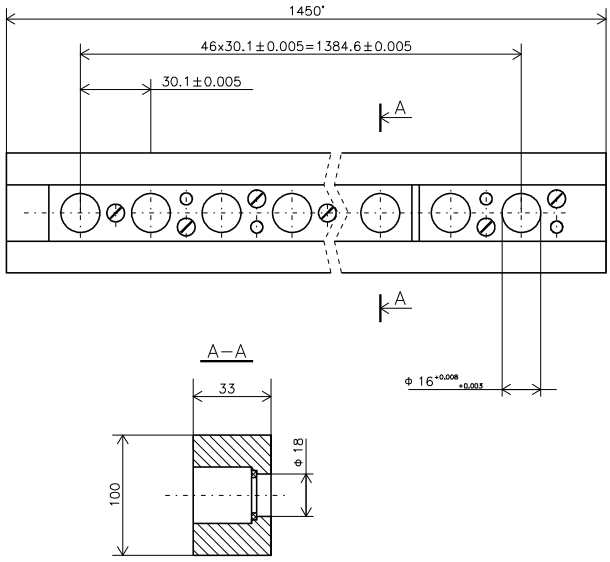

Figure 4: Ball holder (template) for production of precise combs.

This is an aluminium plate with machined cavern of rectangle shape. Steel plates were fixed at bottom of the cavern. The plate length is enough to fix 5 balls except of last one which fixes only two balls. Cuts between the steel plates were done to decrease influence of temperature expansion coefficient difference between steel and aluminium. After fixation of the plates a row of precise holes with precise step was drilled and polished at 20°C. The step of holes was 30.101±0.005 mm with distance between extremal holes 1384.646±0.005 mm. The hole diameter was $16^{+0.008}_{+0.003}$ mm.

For manufacturing of comb the ball holder was placed on flat surface flatness of which was within ±8 μm. Then the holes of the template were filled by balls. A drop of epoxy glue was placed at the top of each ball and the balls were covered by the comb plate. After curing of glue the plate together with balls was removed from the plate holder, rotated and side ditches around the balls (see bottom part of drawing in fig. 3) were filled by final amount of epoxy glue. So, by using **only one** precisely machined template we were able to copy any number of combs.

For the chamber assembling we need 7 combs: 5 combs were placed along chamber with step about 55 cm plus 2 additional combs were used to support ends of short tubes of the chamber cutouts.

After production combs distance between neighbour balls was measured. The distance between balls plus ball diameter is equal to desirable tube pitch in a layer. Dependence of the distance between balls minus 14 mm versus number of gap is shown in fig.5.

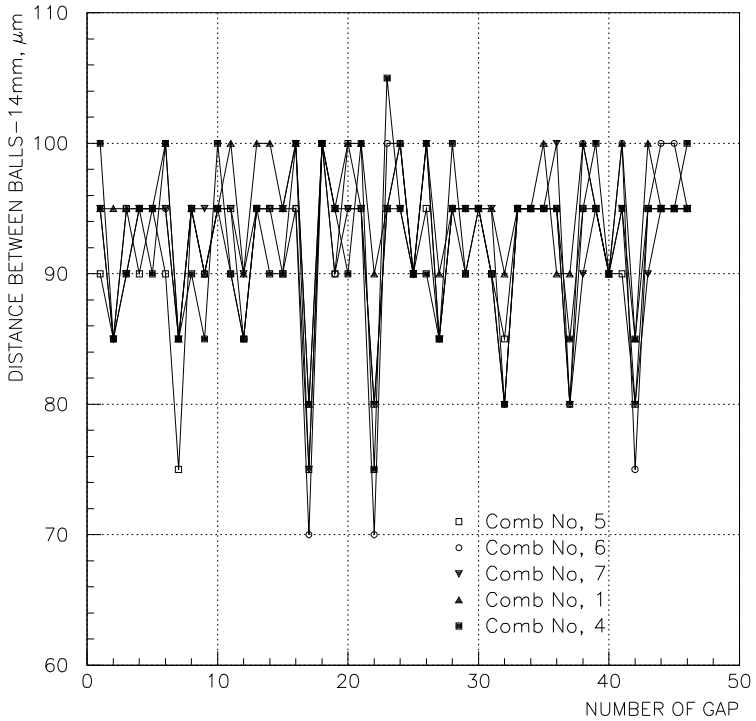

Figure 5: Distance between balls in combs.

In fig.6 histograms of the distance distributions for 5 combs and total one are pre-

sented (horizontal scale units are microns). The mean value of the histogram means step between balls minus 30 mm. Estimated mean value must be 98 μm at 18°C. It is seen that the mean value is smaller. Moreover in fig.5 a regular structure corresponding to steel pieces boundaries in the template is seen also. Both these effects were caused by temperature change during comb production. Temperature was not stabilized and sometimes it was about 15-17^oC.

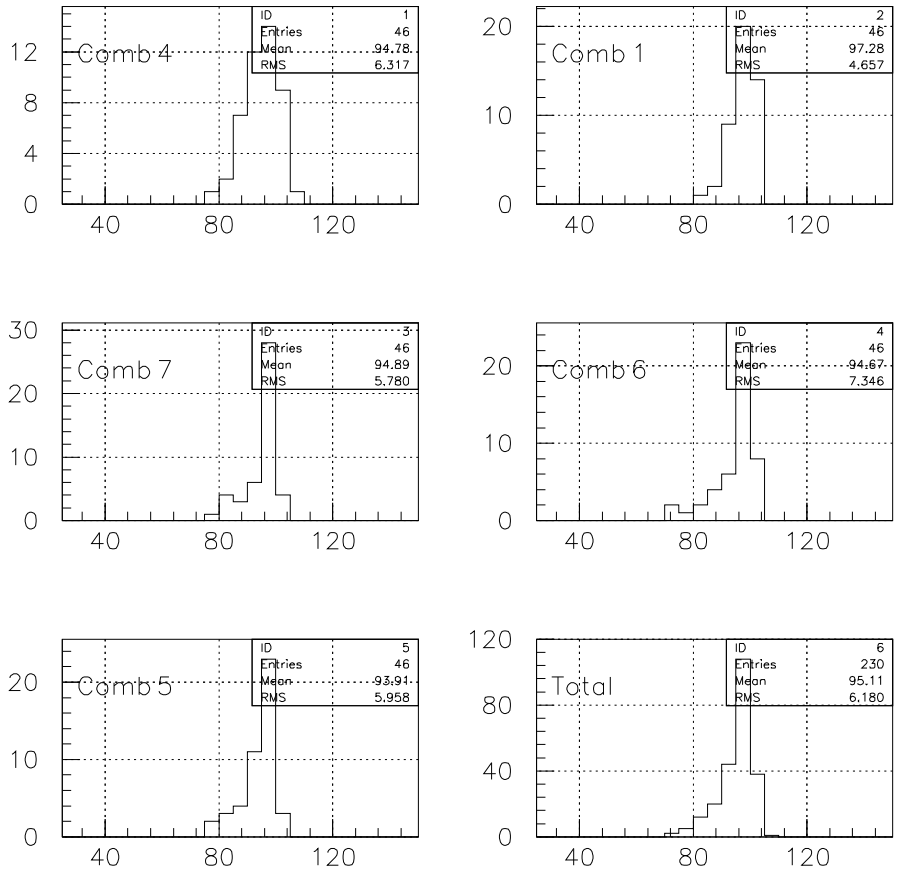

Figure 6: Distributions of distances between balls in combs.

After production of our chamber many people asked us about possible deformation of tubes by balls as soon as a contact between tube wall and ball of the comb are point-like and during gluing of a tube layer a vacuum sucker force is applied to tubes. To answer such question we performed measurements of tube wall deformation and found that it is less than 5 μm with our vacuum suckers (see Appendix 1).

4 Spacer

During design it was considered that the spacer have to support tube multilayers at given distance 150 mm; influence of temperature gradient across chamber have to be minimized; wires must be coaxial to tubes within adopted tolerance (100 μm); in-plane alignment system must be incorporated into the spacer. The spacer is schematically shown in fig.7.

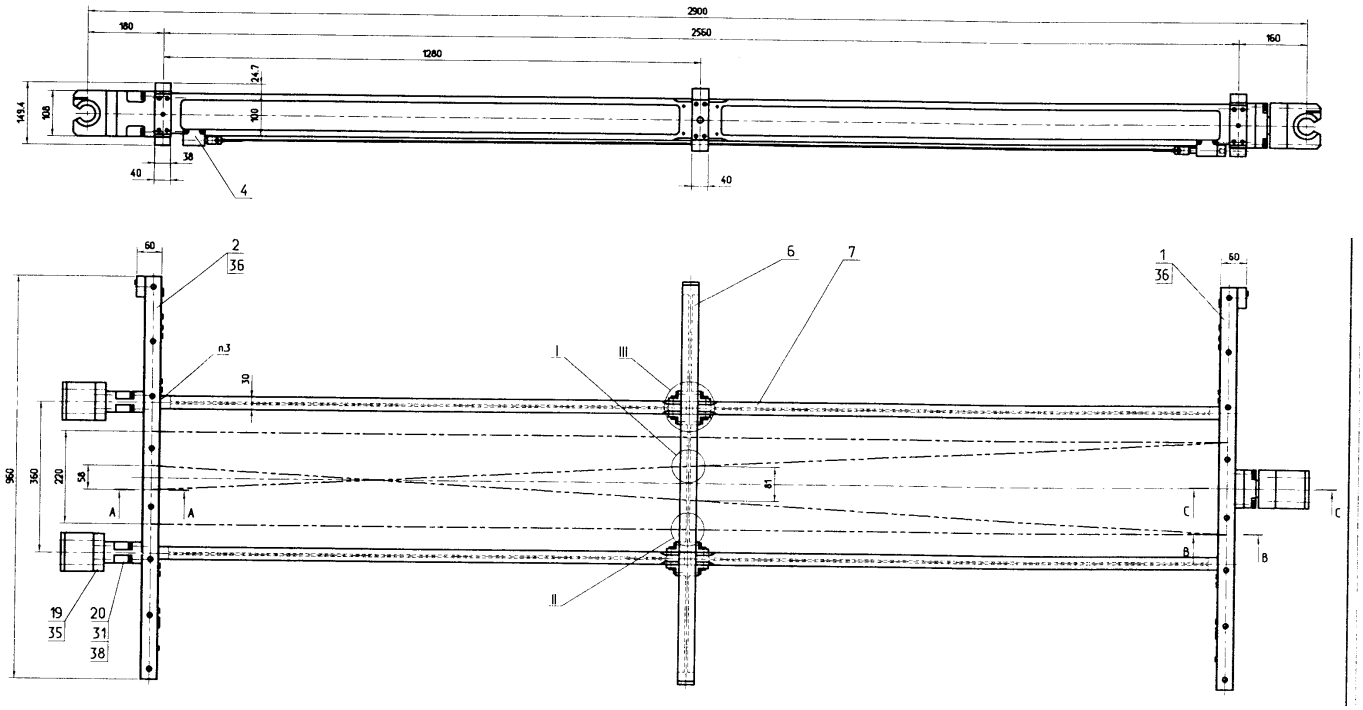

Figure 7: Spacer, side and top view.

The spacer consists of three cross plates transverse to the chamber tubes (marked by digits 2,6,1 in fig.7) and four long beams connecting cross plates. Cross plates and long beams are made of aluminium. Long beam is a machined plate with I-like cross section. Design of cross plate is more complex because of it has to provide flexible connection of multilayers. For these reasons 0.7 mm gap was considered between top and bottom shelves of the spacer and its body (fig. 8.). Unfortunately during assembling of the spacer we forgot about this gap and it was diminished to about zero. About of consequences of this very serious mistake see below in section 7 denoted to chamber sag measurements at DATCHA pit.

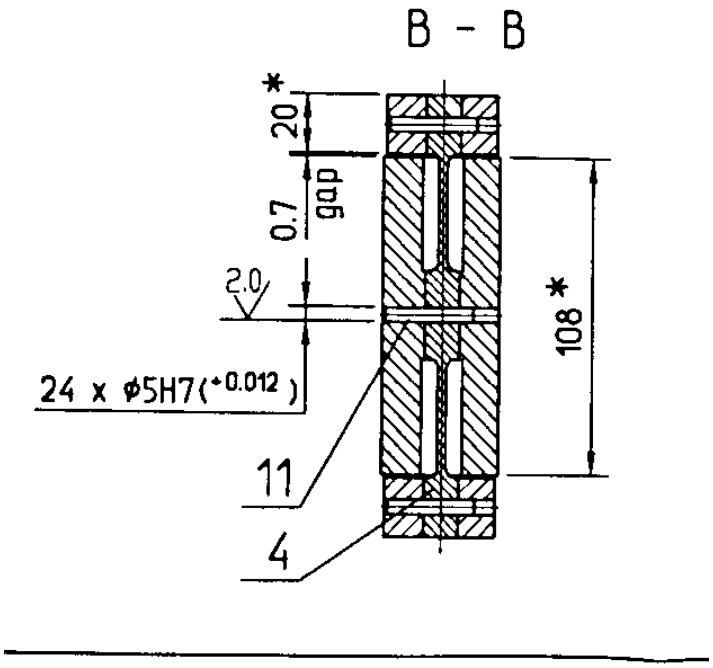

Figure 8: Cross section of side cross plate.

Cross plates also content RASNIK in-plane alignment elements: masks, CCDs and lenses. The alignments rays are shown in fig.7 by long dash-dot lines. Dowel-pins for attachment of DATCHA projective alignment masks were mounted on the extremal cross plates by means of a precise template. 100 μm tungsten wires with tension of 1 kG were stretched through the dowel-pins (along the chamber). The wires were measured during X-tomo scan of the chamber at CERN. It was considered that data of such measurements would be used to connect projective alignment to internal chamber coordinate system.

Estimated values of the cross plate sag is given in table 1.

Table 1. Calculated cross plate sag.

Number of layer	Side cross plate sag,μm	Middle cross plate sag,μm
0	6	7
1	7	8
2	8	9
3	8	10
4	9	11
5	9	12
6	10	13

If the sag of the spacer in transverse direction is negligible the longitudinal one is important. We have to match the sag of wire and sag of chamber to conserve wire-tube

concentricity within of 100 μm. Two tension strips (4 in fig.9) placed under each long beam were considered to adjust the chamber sag to the desirable value. The strip are stretched by screw and can reduce the chamber sag which is initially greater than wire one.

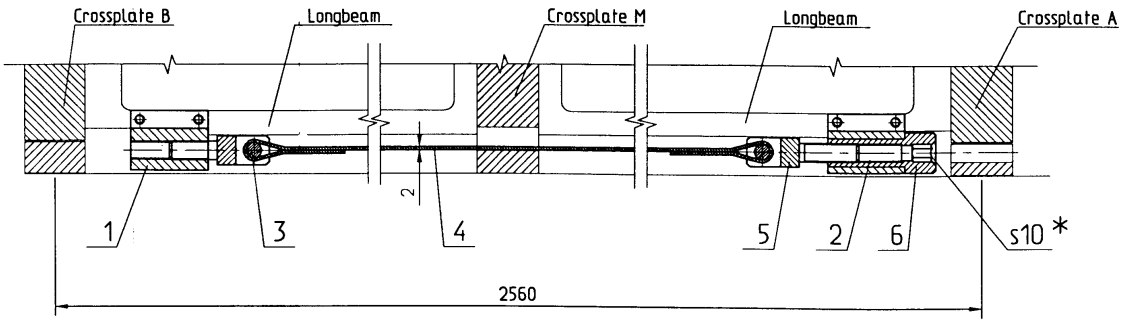

Figure 9: Stretch mechanism of the chamber.

5 Table, combs at table, glue sequence

The tube assembly jig is mounted on a heavy (P=2 tons) steel table with area 880x3800 mm^2. There are 7 combs which are placed on the table. Fig.10 shows one of the combs attached to the table. All combs are identical.

Five combs are distributed uniformly along chamber length. There are also two combs located near ends of short tubes of the chamber. Three rows of vacuum suckers are placed near extremal and middle combs. Combs are mounted on the table when their balls are on the top and under each comb there is a set of screws which allows to adjust comb position in Z- and Y-directions. After mounting combs on the table their positions were adjusted with help of theodolite such that extreme balls of all combs at one side of the table were along a line within of 20 μm and two side lines were in a plane within of the same limit. After chamber assembling the jig alignment was checked again but outstanding of balls from the line and from the plane was not detected within of the mentioned tolerance.

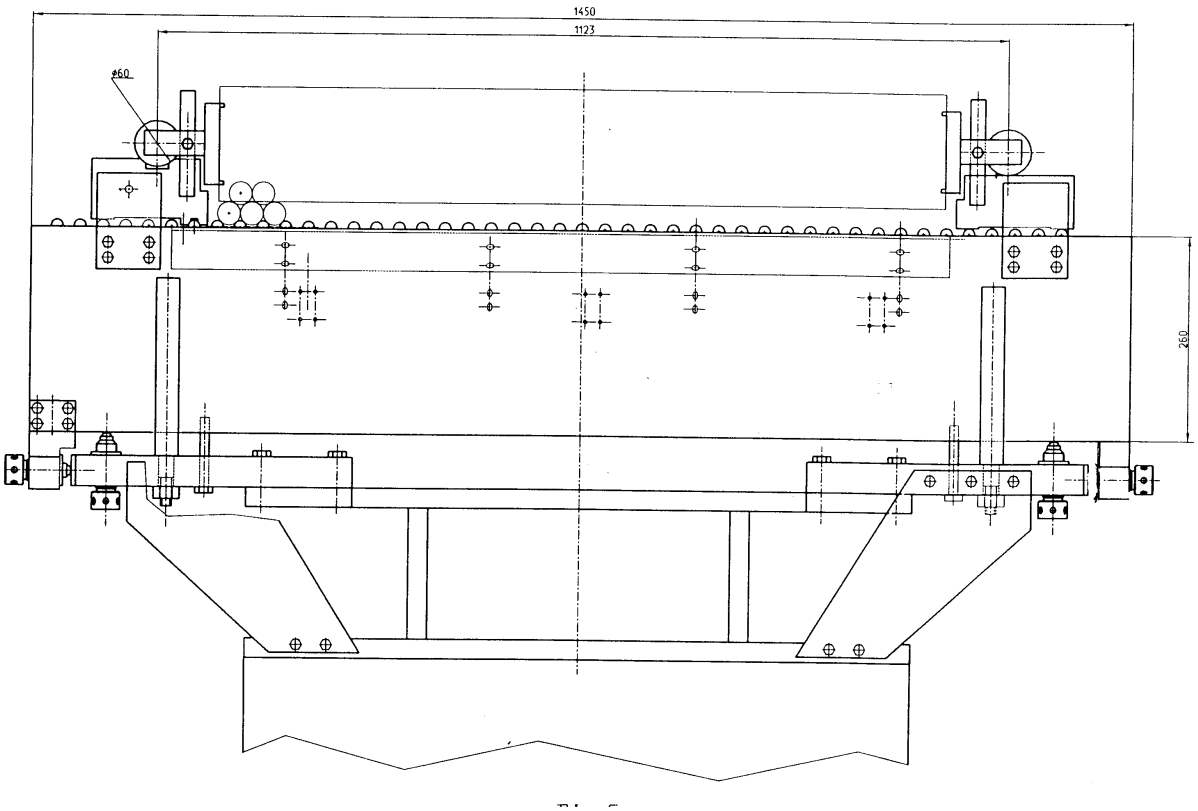

Figure 10: Comb attachment to the assembly table.

During the chamber assembling two balls of 60 mm diameter were temporally attached to sides of each cross plates. Precisely machined steel blocks placed on the combs balls under the temporal balls of spacer were used to fix vertical distance between layers and also horizontal shift of a layer with respect to another. The blocks from one side of the spacer have cylindrical groves corresponding to ball diameter, the blocks of another side have flat top and bottom surfaces. There were 3 sets of such blocks in accordance of number of layers.

Sequence of the chamber assembling was follow. First of all the spacer was assembled and placed on temporal feet above the table for chamber assembling. The first tube layer was placed on combs, vacuum suckers were switched on and epoxy (Araldite 2011) glue strips about 2 mm width were deposited along all tubes at places of their contacts by means of a special glue distributer (fig.11).

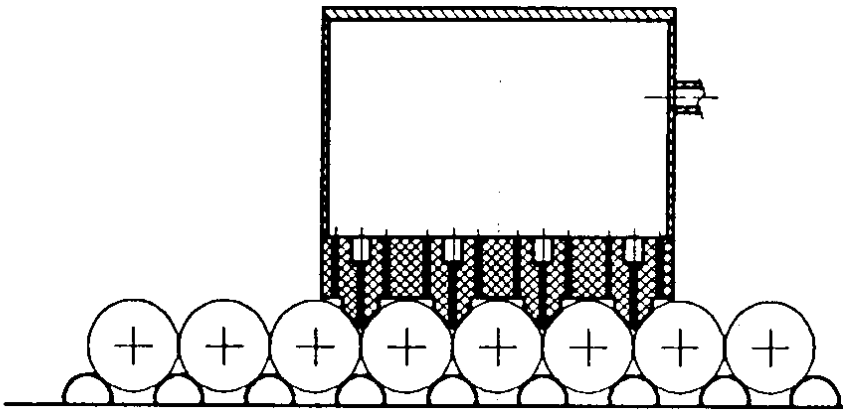

Figure 11: Glue distribution box.

The glue distributer is a box with groves corresponding to the tube pitch at the bottom. There are holes in the bottom of the box above tube contact places. The box is filled by glue. Glue is pushed out of the box by pressure through the holes at the box bottom. To prevent glue flow when the glue distributer is at the end of tubes the gas pressure under glue in the box is changed by vacuum. The box can put glue strips on four tubes simultaneously with speed of about 1 m/min. Deposition of glue strips took about 45 minutes per layer because of we had to fill box several times. After the 1st layer was covered by glue strips the spacer was placed over the layer on precise steel blocks. The distance between tubes and cross plates was 0.3 mm. Triangle like holes between two neighboring tubes and cross plate surface were filled by special shape aluminium pieces and glue. After curing of glue the spacer with the 1st layer was raised up at temporal feet, new layer of tubes was placed on ball combs, covered by glue, precise steel blocks were changed and spacer with the 1st already glued layer was attached to the second layer. Such operation was repeated 6 times. After gluing of the 3d layer the spacer was rotated around X and Y axis to conserve the same reference side for both multilayers.

There were two accidents during the gluing of the 3d layer. Due to error in precise blocks we had to keep the layer in semi-glued position about 10 minutes and in half an hour after attachment the layer to previous one vacuum pump of the suckers was broken. The glue curing of the layer was continued without vacuum suckers but we put weight distributed at every end plug to secure normal position of tubes in the layer.

6 RASNIK measurements during the chamber assembling

As was told before the RASNIK system of four lenses, four LED illuminated masks and two CCD was included in the chamber spacer. We did some measurements with such system during the chamber assembling.

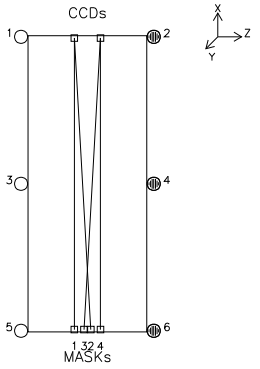

Figure 12: RASNIK rays scheme.

For each alignment ray (fig.12) we measured relative change of mask image at CCD. Initial position of the image was taken for free spacer on the assembling table. We shall show only several more typical results concerning the chamber gluing history as it was seen by RASNIK system. Example of such temporal dependence for RASNIK ray number 1 is shown in fig.13.

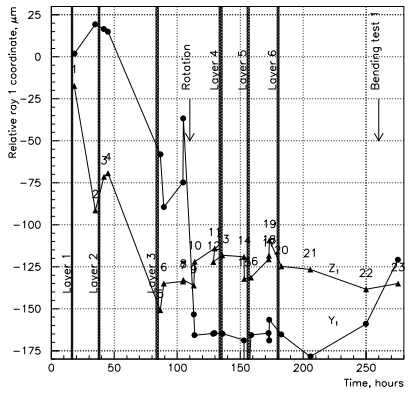

Figure 13: BIL chamber assembling history.
RASNIK/CCD beam 1 Y- and Z-coordinate.

Hatched strips in fig.13 denote time of gluing of layers, arrows indicate rotation of the chamber and time of a bending test which was performed after finishing of the chamber gluing. Digits near points denote sequential number of measurement. After completion of the 3d layer change of vertical and horizontal positions of the image (DY and DZ) is about 70 μm and 110 μm accordingly. DY reduced to 40 μm when 80 kg weight was removed from top of the chamber (points 7,8). After rotation of the chamber DY became 170 μm with respect to initial 0. Difference DY before and after bending test is about 45 μm. All these indicate presence of an imperfection in our chamber. We suppose that it could be caused by our error during cross plate assembling (see above about 0.7 mm gap, fig.8).

In fig.14 we present the Y-,Z-coordinate difference of two RASNIK beams 1 and 4 which are more sensitive to a torsion of the chamber.

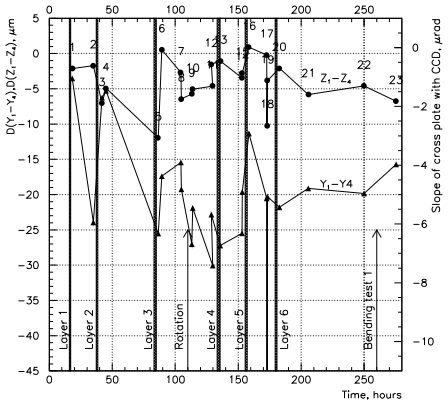

Figure 14: BIL chamber assembling history.
RASNIK/CCD beams difference sensitive to a torsion.

There is a torsion of about 100 μrad.

We also performed some bending tests of the chamber.

The 1st one is increasing of the height of supports under balls 1,2 (see fig.12). The test was combined with simultaneous torsion test when we did difference of height supports 1 and 2 equal to ± 80 μm corresponding to inclination of the cross plate ± 72 μrad. Examples of results are presented in fig.15,16.

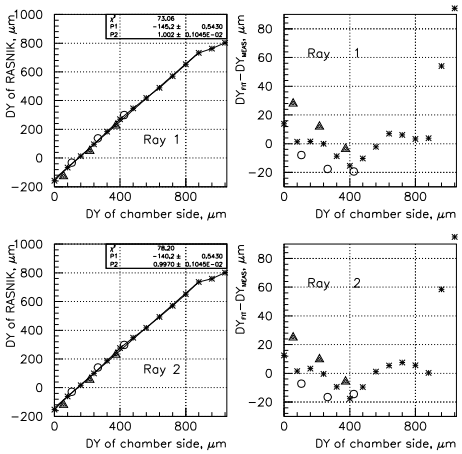

Figure 15: RASNIK rays 1 and 2
Y-coordinate vs. bending
of CCD chamber side.

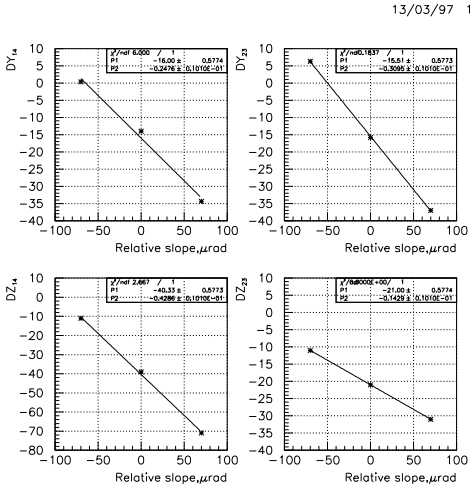

Figure 16: RASNIK rays 1-4 and 2-3
difference vs. slope of
cross plate with CCD.

Fig.15 shows Y-coordinate of ray 1 vs. height of CCD chamber side with linear fit. Crosses, triangles and open cycles correspond to inclination of cross plate 0, -72 μrad and $+72$ μrad. The change of slope dependence of Y vs. height is well seen. It corresponds to disconnection of middle balls of the spacer from supports. This is direct measurement of

the chamber sag which is 440 μm. Unfortunately the measurements were done for rotated (top-bottom) position of the chamber.

7 Chamber sag compensation test and chamber twist measurements

Test of the BIL chamber stretch mechanism was performed after installation of the chamber into DATCHA pit by using of stretched wires. Tungsten wires with the same parameters as for wires used in drift tubes were stretched above the chamber (fig.17).

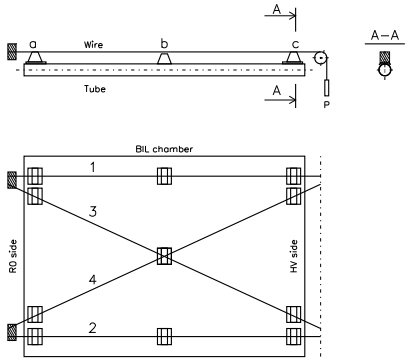

Figure 17: Scheme of stretched wires over the chamber.

Two precise prisms ('a' and 'c') fixed wire vertical position at a tube ends. Mylar films of 20 μm thickness were placed under the prisms to prevent electrical contact between them and the tube. The films under 'c'-prism were used simultaneously to regulate Y-coordinate of the prism. We tried to fix the beginning of an electrical contact between the wire and prism 'b' placed at middle of the tube. We estimated that the accuracy is about of 20 μm for such measurements.

Wires 1 and 2 were used to measure sags for two sides of the chamber when the stretch mechanism was switched on and off. Results are given in Table 2 where differences of the chamber side sag and one of the wire are given.

Table.2 Sag difference ($Sag_{chamber}$-Sag_{wire}),μm

	Wire 1	Wire 2
Chamber was not stretched	0	200-250
Chamber was stretched	-65	0

Wires 3 and 4 were used to measure the chamber twist after switch on the chamber stretch mechanism. We measured 50 μm vertical distance between wires 3 and 4 in their intersection point. The value corresponds to 80 μm torsion for full chamber width 960 mm.

From the measurements we concluded that stretch mechanism does not provide a correct compensation of the chamber sag and the chamber twist is too big. The most probable cause of these shortcomings is an error during the spacer assembling (see fig.8, 0.7 mm gap which was not done).

8 X-tomography results

It is evident that X-tomo existing results have systematics. The most evident indications of the systematics in 2D data are:

1. $\sim$-like behaviour of Y-coordinates of wires in a layer especially in layers which are far away from X-tomo calibration ruler;

2. all tested chambers look like parallelogram, inclination of vertical wire rows from perpendicular is about 0.4-0.6 mrad.

But in any case the present X-tomo data are very interesting and must be analyzed.

Here we shall present some our points of view on two-dimensional X-tomo data taken from Yu.Sedykh.

Table 3. X-tomo 2D-analysis data and chamber Z-pitch.

Producer of chamber	Data file name	Z-pitch,mm
Roma-Pavia	Wires_Coord_roma2np.dat	30.01
Frascati	Wires_Coord_frascati4np.dat	30.05
Protvino	Wires_Coord_protvino1np.dat	30.10
Protvino	Wires_Coord_protvino2np.dat	30.10

. We performed very simplified analysis. We did not use the program of "stretching" a regular 2D grid for measured points like in work [8], because of using such method for systematically shifted data can produce more systematics.

The first of all we should like to pay attention to the presence of cutouts for projective alignment in Protvino chamber (see fig.1). Tension of wires in short tubes of the cutouts was chosen such that the sag of short tube wires must be the same as of long tubes one but during X-tomography scan of the chamber the stretch mechanism was not switch on and there was difference in relative Y-coordinate of long and short tube wires due to the chamber sag. It is clearly seen in fig.18 where difference of wire Y-coordinate from mean value is shown for each layer. Black hatched bins in three upper layers correspond to short tubes, dot-hatched bins are long tube wires. Mean value of the difference is 68.5 ± 23(RMS) μm for scan at middle and 55.3 ± 29(RMS) μm for scan near HV end of the chamber. For correction of short tube wire Y-coordinate we used measured value of the chamber sag 440 μm (see section 6). After the correction the mean outstanding of Y-coordinate of short tubes became about several microns.

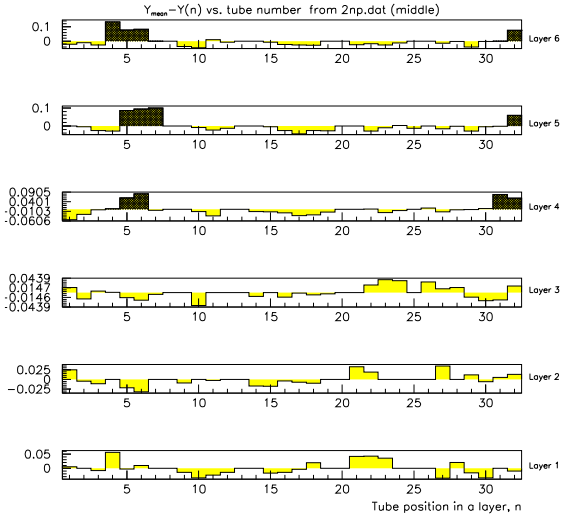

Figure 18: Y_{mean}-Y_n vs. tube position (n) in a layer.

In each layer we calculated RMS of wires Y-coordinate distribution. Results are given in fig.19 as a function of vertical distance between a layer and X-tomo head. The drawing shows also the X-tomo systematics influence.

For calculation of wires Z-pitch we used separately in each layer the 1st order polynomial fit Z=p0+p1·N, where N is a tube position (number) in a layer. In fig.20 RMS of wire Z-coordinate with respect to the fitted line is presented.

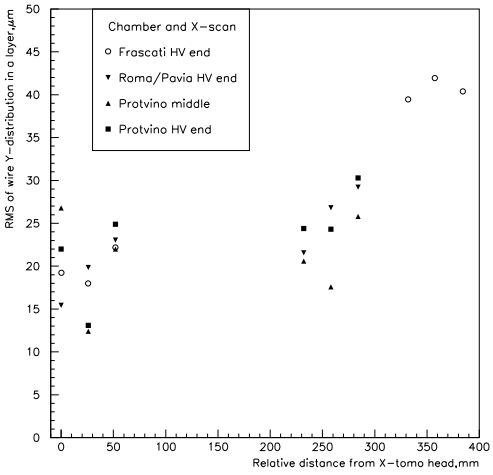

Figure 19: RMS_Y vs. distance from X-tomo.

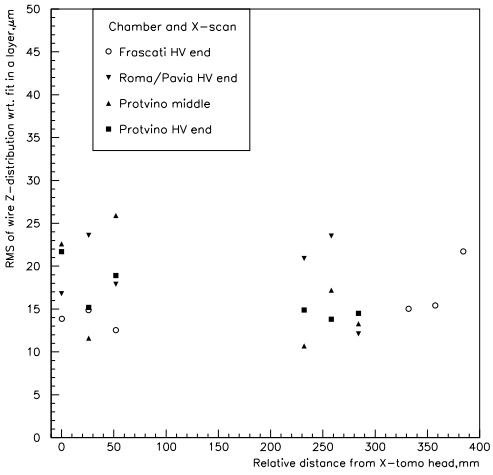

Figure 20: RMS_Z vs. distance from X-tomo.

From the fit line it is possible very precisely (error of fit parameter p1 is about of 0.3 μm) to estimate Z-pitch of wires within a layer. In fig.21 difference of the measured and predicted Z-pitch (see table 3) is shown as a function of vertical distance from X-tomo head.

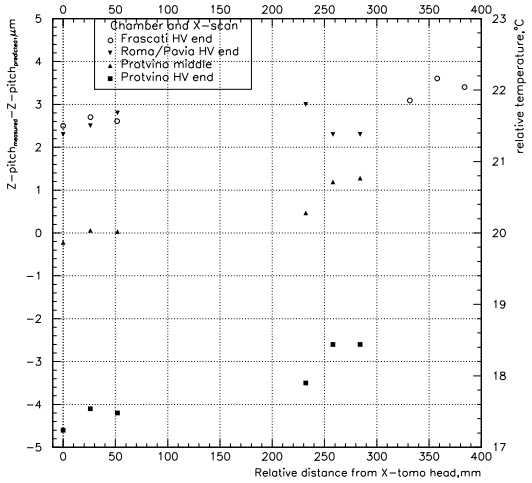

Figure 21: Z-pitch$_{meas}$-Z-pitch$_{pred}$ vs. distance from X-tomo.

At right side of the dependence we placed relative temperature scale because there is an indication of pitch difference between top and bottom multilayer which can be attributed to presence of temperature difference between multilayers or some systematics. Unfortunately we can not answer who is responsible for the systematics: X-tomo or assembling tools.

During X-tomo scan of the chamber one broken wire was detected. The wire disconnected from HV side and was not detected our simplified HV test of tubes [2]. Because of this reason we can not answer the question when wire was broken, before or after the chamber shipment.

It is seen that wire location within a layer is better than 20-25 μm. This is upper estimation including X-tomo errors. Existing X-tomo precision do not permit to answer the question what chamber and what technology are better.

9 Very preliminary results of cosmic-ray test

After installation of the chamber in DATCHA pit some preliminary cosmic-ray tests were done. They show that the chamber works properly without dark current and noise. With Ar-CO_2=87-23 mixture at 2.1 bar pressure and limited number of readout electronic channels (32) residuals distribution about 80 μm was measured. Measurements with DATCHA electronics are only starting. In fig.22 drift time spectrum mixture for all wires is shown. The spectrum was measured with DATCHA electronics and Ar/CO_2 gas.

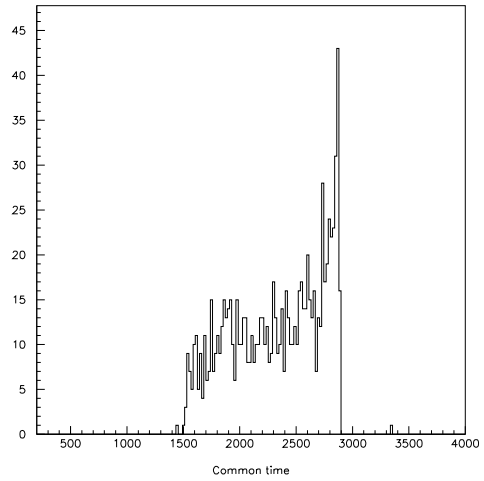

Figure 22: Drift time spectrum.

Distribution demonstrates absence of any background and noise. Preliminary test indicates that there is at least one wire without electrical contact additionally to one detected during X-tomo scan.

10 Conclusions

Full scale prototype of MDT-BIL chamber has been built in IHEP of Protvino using layered approach. The chamber is not free from disadvantages, during its construction we did mistakes, some of them have been already fixed. But in any case we can conclude that we are able to construct properly working large chamber when precision of wire location within a layer is not worse than 20-25 μm.

References

[1] ATLAS Technical Proposal. CERN/LHCC/94-43.

[2] A.Borisov et al. Wiring of tubes for full scale BIL chamber prototype. ATLAS Muon Note 143

[3] H.Bilokon et al. MDT Chamber precision Assembly, ATLAS Muon Note 081.

[4] The MDT endplugs ATLAS MUON Note 181.

[5] C.Daly et al. Concept for the Design and Assembly of Forward Region MDT Chambers for ATLAS. ATLAS MUON Note 086.

[6] A.Manz et al. Mechanical Stacking of Muon Drift Tubes into Modules. ATLAS MUON Note 123.

[7] P.Benvenuto et al. MDT chamber assembly procedure and construction of a full scale BML. ATLAS MUON Note 152.

[8] F.L.Linde & G.G.G.Massaro. Grid fits for BIL X-tomography data. ATLAS MUON Note 188.

Appendix 1.

Measurements of tube deformation by balls of comb

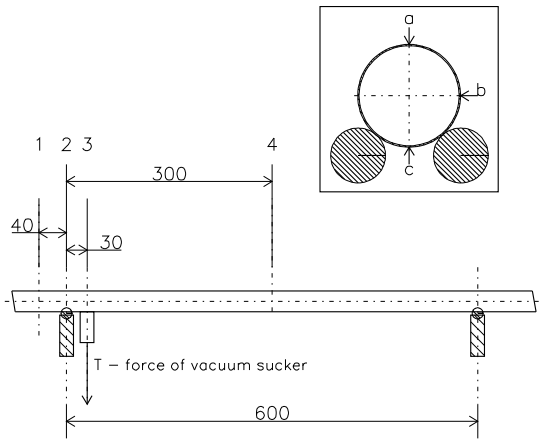

Figure 1: Scheme of ball-tube deformation test.

Scheme of measurements is shown in fig.1. Cross section of a tube perpendicular to its axis at middle of balls is shown in right corner. Outer ball diameter is 16 mm. Distance between balls is 30.1 mm. Tested tube was produced by METALBA, OD=30 mm, wall thickness is 0.4 mm. Arrows indicated by letters 'a','b','c' denote points of attachment of measurement gauge. Cross section along a tube axis is shown between two consequent combs. Digits '1','2' and '4' indicate position of gauge, '3' is vacuum sucker position. So, the position of gauge is denoted by a digit and letter, e.g. '1a'. We measured a change of position tube wall under vacuum sucker force. Precision of the gauge was about 2 μm.

Results of the measurements are given in fig.2. Fig.2 shows superimposed results for measurements in points '1c', '1a', '2b', '2a' and '4a'. Sign of height change was inverted. Measurements at point '2b' give us zero side displacement.

Conclusion. We explored vacuum suckers force 0.6 kG during assembling BIL prototype. For such force of the suckers the largest tube deformation (at bottom of tube between balls) is less than 5 μm.

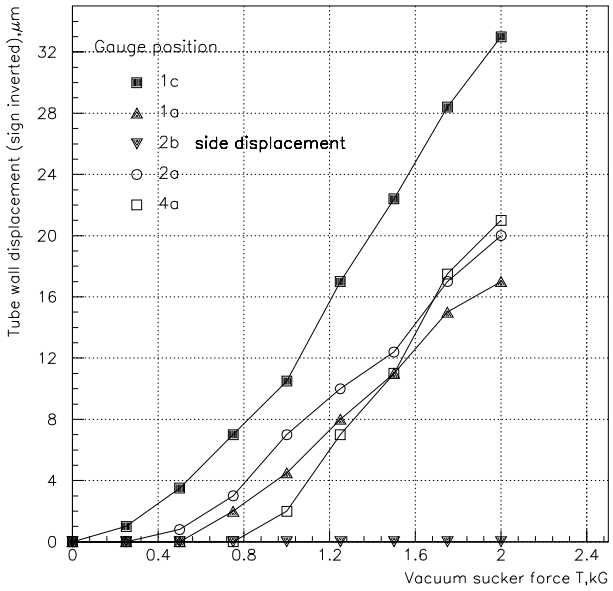

Figure 2: Tube deformation at different points under vacuum sucker force.